PERFORMANCE SENSITIVITY ANALYSIS OF DEPARTMENT OF ENERGY — CHRYSLER UPGRADED AUTOMOTIVE GAS TURBINE ENGINE (S/N 5-4)

Roy L. Johnsen
National Aeronautics and Space Administration
Lewis Research Center

December 1979

Prepared for
U.S. DEPARTMENT OF ENERGY
Conservation and Solar Applications
Transportation Energy Conservation Division

NOTICE

DOE/NASA/1040-79/9
NASA TM-79242

PERFORMANCE SENSITIVITY ANALYSIS OF DEPARTMENT OF ENERGY - CHRYSLER UPGRADED AUTOMOTIVE GAS TURBINE ENGINE (S/N 5-4)

Roy L. Johnsen
National Aeronautics and Space Administration
Lewis Research Center
Cleveland, Ohio 44135

December 1979

Work performed for
U. S. DEPARTMENT OF ENERGY
Conservation and Solar Applications
Transportation Energy Conservation Division
Washington, D. C. 20545
Under Interagency Agreement EC-77-A-31-1040

SUMMARY

Performance sensitivities and interactions between gas turbine engine components were examined analytically when changes were made to several significant component performance and operating parameters. The gas turbine engine, a two-shaft configuration called the Upgraded engine, was developed by the Chrysler Corporation under a U.S. Department of Energy contract. The early Upgraded engines had a serious power shortfall, and a cooperative effort was undertaken to remedy the problem. One aspect of the corrective action program was an engine test at the NASA Lewis Research Center of one of the early Upgraded engines. To provide additional support for that test the engine was analytically modeled for use with a performance prediction computer code. The code had the flexibility to permit the incorporation of details such as the turbomachinery maps and other actual test data relative to component performance. The performance sensitivity was examined for changes to several operating and component performance parameters. One change at a time was introduced, and the performance was calculated and then compared to the reference performance. This comparison was made at gas generator speeds from 50 (idle speed) to 100 percent. Sensitivities were determined for changes in turbomachinery efficiency, compressor inlet temperature, power turbine discharge temperature (which was actively controlled), regenerator effectiveness, regenerator pressure drop, and several gas flow and heat leaks.

As expected, the efficiency of the compressor and the turbines strongly affected performance. Compressor efficiency, which had the strongest effect on system performance, was closely followed by compressor-drive turbine and power turbine efficiencies. Efficiency changes to either the compressor or compressor-drive turbine efficiencies resulted in a shift in the operating point of the other two machines. For constant shaft speeds and power turbine discharge temperature, increasing the compressor efficiency resulted in reduced pressure ratio for the compressor-drive turbine and increased pressure ratio for the power turbine. Changes to power turbine efficiency did not affect the operating point of the other two machines. A tabulation of influence coefficients for several dependent variables is included for gas generator speeds from 50 to 100 percent.

INTRODUCTION

The Upgraded gas turbine automotive engine development program was initiated by the Environmental Protection Agency in 1972 with a multi-year contract to Chrysler Corporation. The U.S. Department of Energy, after its formation, took over the program and in 1977, while continuing direct funding, transferred the technical management responsibility to the NASA Lewis Research Center Gas Turbine Project Office. A power shortfall in the first engines resulted in an intense corrective action program. Chrysler and its contractors undertook component redesign to correct the power deficiency. Included in the corrective action program was some diagnostic testing. One of the early Upgraded engines (serial no. 5-4) was tested at Lewis (ref. 1 and unpublished Lewis data by Horvath, Ribble, Warren, and Wood). To support that test effort a sensitivity analysis was done to determine the influence of the more important component parameters. The performance of engine 5-4 was poor with peak measured power of about 38.8 kilowatts (52 hp) instead of the goal of 77.6 kilowatts (104 hp). Initially the Lewis test engine encountered combustion instability at the higher gas generator speeds although no problems were encountered at 80-percent speed or less. The performance figures reported herein are for engine 5-4, one of the early engines. For engine 5-4, the maximum power attainable was about 50 percent of the design goal. Corrective action by Chrysler has brought the current Upgraded engine power up to about 87 percent of the design goal.

The Chrysler Upgraded engine (S/N 5-4), a two-shaft regenerated engine, was modeled mathematically using a gas turbine engine performance computer code designated N.N.E.P. (Navy-NASA Engine Program). The N.N.E.P. version used was specifically adapted to automotive gas turbine engine applications. With this code, influence coefficients were determined for the effect of compressor efficiency, compressor-drive turbine efficiency, power turbine efficiency, regenerator effectiveness, regenerator pressure drop, parasitic power losses for the gas generator shaft and power turbine shaft, various flow and heat leaks, compressor inlet temperature, and power turbine discharge temperature.

SYMBOLS

A	auxiliary and parasitic power losses
N	rotational speed
p	pressure
$(\Delta p/p)$	pressure drop fraction

q_l	heat leak
SFC	specific fuel consumption
T	temperature
x	independent variable
y	dependent variable
$(\dot{\omega}_l/\dot{\omega}_a)$	flow leak fraction
η	component efficiency

Subscripts:

a	air
a_1	air at station 1, fig. 1
c	compressor
ct	compressor-drive turbine
f	fuel
GG	gas generator shaft linking compressor with compressor-drive turbine
l	leak
pt	power turbine
ref	reference
reg	regenerator
std	standard or reference value
$4 \rightarrow 33$	typical nomenclature for flow leaks; in this case, duct 4 to station 33 in fig. 1

ANALYTICAL MODEL AND COMPUTER CODE

The information required to analytically model the Upgraded engine was obtained from Chrysler Corporation and from tests at the NASA Lewis Research Center. The compressor and turbine maps were obtained from cold flow tests conducted at Lewis. The compressor map was obtained from a rig test of the actual Upgraded compressor (ref. 2). Maps for the two Upgraded turbines were not available when the analysis was originally conducted. However, the turbines for a larger but similar engine, the Chrysler Baseline engine, had been tested at Lewis (refs. 3 and 4). The Chrysler Baseline and Upgraded engines were both two-shaft engines with the power turbine having variable nozzle vanes for control. The Chrysler Baseline engine was a 111.8-

kilowatt (150-hp) engine, while the Chrysler Upgraded engine had a design goal of 75 kilowatts (100 hp). Because of the similarities between the two engines, the Baseline turbine maps were scaled for the Upgraded sensitivity study. After the Upgraded turbine maps from rig tests became available, sensitivity calculations were repeated for the independent parameters which caused the map operating points of the turbomachinery to shift. Thus, the sensitivity calculations to determine the effect of compressor efficiency, compressor-drive turbine efficiency, power turbine efficiency, compressor inlet temperature, and controlled power turbine discharge temperature were repeated using the Upgraded turbine maps. Calculations were not repeated for the effect of heat leaks, flow leaks, regenerator effectiveness, regenerator pressure drop, and parasitic losses. The original intent was to match design performance to the original Chrysler performance goals at the rated power. But at that time engine 5-4 on test at Lewis was unable to run at 100-percent gas generator speed because of combustion instability. Therefore, the turbine map operating points at 80-percent gas generator speed and power turbine speed of 30 800 rpm were matched to actual test data for engine 5-4. In addition to the compressor and turbine maps, data from the same tests were used to estimate total pressure losses for the compressor diffuser and for the ducting between the two turbines. Predictions by Chrysler were used for the reference values for flow leakage magnitudes and their flow paths, heat leak magnitudes and flow path, inlet duct total pressure recovery, combustion efficiency, combustor pressure drop, regenerator effectiveness, regenerator pressure drop for both high and low pressure sides, and parasitic power losses for the gas generator shaft and the power turbine shaft.

The computer code used was a version of the N.N.E.P. (ref. 5), which had been specifically adapted for ground transportation gas turbine engines. The code enables modeling with a building block approach. Figure 1 shows a block diagram of the engine component arrangement showing physical linkage components and gas flow paths. The assumed leakage flow paths and leakage rates estimated by Chrysler (ref. 6) were used for this analysis. The gas generator shaft links the compressor with the compressor-drive turbine. The load on the gas generator shaft is not a mechanical component but a means of introducing shaft bearing and windage parasitic losses. The power turbine shaft shows only a turbine and a load which would be input power to a transmission after parasitic losses were subtracted. The computer code permits specifying turbomachinery maps, pressure drop fractions as a function of corrected flow, heat losses and flow leak losses, parasitic losses for the shafts as a function of rotational speed, and component efficiencies (such as combustion efficiency and regenerator effectiveness) as a function of some applicable variable such as corrected flow. The mathematical model was valid for steady-state operation only; transient operation was excluded.

DISCUSSION OF RESULTS

Sensitivities were determined at discrete operating points on the engine map shown in figure 2. Sensitivities were evaluated primarily by examining influence coefficients. The influence coefficient is the fractional change of the dependent variable divided by the fractional change of the independent variable. In figure 2 the engine power is plotted against the propshaft speed for a series of gas generator speeds from 50 to 100 percent of design. The propshaft speed is related to power turbine rotational speed through a 14.89 gear reduction. For a given gas generator speed there is a power turbine shaft speed where output power is maximum. The sensitivities were determined at these optimum operating points (solid triangular symbols in fig. 2).

The sensitivities were determined for the entire list of independent variables using the scaled Baseline turbine maps. When rig test maps for the Chrysler Upgraded turbines became available they were incorporated in the analytical model. Subsequently, calculations to determine sensitivity to the efficiency of the compressor, compressor-drive turbine, and the power turbine were repeated. Sensitivities to compressor inlet temperature and power turbine discharge temperature were also recalculated. Sensitivities to all other independent parameters were determined only for the model containing scaled Baseline turbine maps. For the turbomachinery efficiencies both sets of influence coefficients are shown in the plots and in the appendix.

The shaft speeds for the gas generator and the power turbine were held constant when determining these sensitivities. Also, the power turbine discharge temperature was held constant by controlling the position of the power turbine nozzle vanes. The power turbine nozzle control is the normal control mode for the actual engine and was simulated for the analytical study. The independent variable delta was 1 percent for the turbomachinery at the 80-percent speed match point. The appendix lists the magnitude for each independent variable.

Effect of Turbomachinery Efficiencies

Improving the efficiency of one of the turbomachines may affect the operating points of the other two machines. A compressor efficiency improvement results in reduced compressor work, and this then results in a reduced pressure ratio for the compressor drive turbine. This in turn results in a higher pressure ratio for the power turbine. The effect of compressor efficiency on the turbine operating point is shown in the turbine maps of figure 3. The ordinate of the map is specific turbine work, and the abscissa is the speed - mass flow parameter, which is simply the product of corrected speed and corrected flow. The compressor map is not shown, but after rematching the compressor pressure ratio was slightly higher and the air flow was slightly lower. The

compressor-drive turbine in response moved along a constant speed line to a lower pressure ratio and slightly higher efficiency. The lower pressure ratio of the compressor-drive turbine resulted in slightly higher temperature and pressure at the inlet to the power turbine. Thus, a compressor efficiency increase moved the power turbine operating point to a higher pressure ratio, slightly lower efficiency, and slightly lower corrected speed.

For an increase in compressor-drive turbine efficiency the match points of all three turbomachinery components were affected in a similar fashion. Compressor pressure ratio and efficiency increased slightly, compressor-drive turbine pressure ratio decreased, power turbine pressure ratio increased, and efficiency decreased.

The effect of increased power turbine efficiency was an exception. The operating point of the compressor and compressor-drive turbine was shifted very little when the power turbine efficiency increased.

Sensitivity to Compressor Efficiency

The effect of compressor efficiency on specific fuel consumption (SFC) and engine net power is shown in figure 4 for a gas generator speed of 80 percent. The reference compressor efficiency obtained from testing was 0.741. The efficiency was reduced to 0.733 for the low limit and increased in increments to a high of 0.805, which was the Chrysler original design goal at 80-percent gas generator speed. The compressor turbine and power turbine were treated as fixed components; this required that the turbine operating points rematch in response to the compressor performance changes. In figure 4, net engine power increased almost linearly with increases of compressor efficiency. The slope of the line at 0.741 is related to the influence coefficient of compressor efficiency on net engine power. The influence coefficient for power can be thought of as the percent change in horsepower for each percent change in compressor efficiency. The power and SFC influence coefficients at 80-percent speed are shown in figure 5. The 80-percent speed is where the analytical results were matched to the results from the Lewis test facility. The remaining points were influence coefficients obtained at other off-design points at other gas generator speeds. Two sets of influence coefficients are shown. The triangular symbols indicate that actual Upgraded turbomachinery maps were used in the analytical model, and circular symbols indicate that scaled Baseline turbine maps were used. The influence coefficients are basically in agreement from 70- to 90-percent gas generator speed. From 70 to 90 percent the engine power changed about 2 percent for a 1-percent compressor efficiency change. Below 70-percent and above 90-percent gas generator speed the sensitivity to compressor efficiency improvement is greater. The model underpredicted the influence of

compressor efficiency at low and high gas generator speed when the scaled turbine maps were used. With the Upgraded turbine maps in place, the power and SFC were quite sensitive to compressor efficiency at low speed idle and high speed. In addition to the influence coefficients of power and SFC shown in figure 5, the appendix tabulates influence coefficients for all of the dependent variables to compressor efficiency changes at several gas generator speeds. The appendix shows in detail how the pressure ratio and efficiency of the turbomachines respond to the compressor efficiency change. In addition, effects on fuel consumption, airflow, and several engine temperatures are shown. The use of the influence coefficients is also illustrated in the appendix.

Sensitivity to Efficiency of the Compressor-Drive Turbine

The effect of compressor-drive turbine efficiency on engine power and SFC at 80-percent gas generator speed is shown in figure 6. The reference total efficiency was 0.745 as determined from tests. The efficiency range covered was from 0.737 to an upper limit of 0.843. The engine power plotted against turbine efficiency (fig. 6) was not linear as in the case of compressor efficiency. The sensitivity as seen from the slope of the line was greater at the lower end of the efficiency range. The influence coefficients for power and SFC at the reference efficiency of 0.745 are shown in figure 7 for 80-percent speed. For the 70- to 90-percent speed range, the increase in influence coefficient for power was between 1.9 and 2.3 percent for each 1-percent increase in compressor-drive turbine efficiency. Figure 7 includes the influence coefficients at other speeds as determined from off-design calculations. Again two sets of influence coefficients are shown with the set marked Upgraded turbine maps being preferred. The two sets are in basic agreement between the 70- and 90-percent gas generator speeds. The sensitivity to compressor-drive turbine efficiency is greater at the low and high ends of the gas generator speed range. At 50-percent speed the power increased more than 8 percent for each percent improvement of turbine efficiency. Influence coefficients for SFC are shown in the upper part of figure 7. The SFC is reduced about 1.75 percent for each percent increase in compressor-drive turbine efficiency. The appendix shows for 80-percent speed that the compressor operating point has changed to a slightly higher compressor pressure ratio, slightly higher compressor efficiency, and lower airflow. The improved compressor-drive turbine efficiency meant that required turbine work could be obtained with a pressure ratio lowered by 0.6 percent for a 1-percent improvement in compressor-drive turbine efficiency. The decrease in compressor-drive turbine pressure ratio resulted in a higher pressure to the power turbine. The 1-percent compressor-drive turbine efficiency improvement

resulted in a 0.7-percent increase in the power turbine pressure ratio with power turbine efficiency 0.9 percent lower. However, the net result was an increase in power of 1.9 percent. The magnitude of the influence coefficient for power indicates a sensitivity to compressor-drive turbine efficiency about the same as sensitivity to compressor efficiency.

Sensitivity to Power Turbine Efficiency

The effect of power turbine efficiency on engine power and SFC is plotted in figure 8. The range of power turbine total efficiency covered was 0.651 to 0.755. The reference total efficiency at 80-percent gas generator speed was 0.661 (rated from stator inlet to diffuser outlet). The power changed approximately linearly with power turbine efficiency. The SFC variation is not linear, being slightly more sensitive to power turbine efficiency at the lower end of the efficiency range. Two sets of influence coefficients are shown in figure 9 for the effect of power turbine efficiency on power and SFC. The preferred set used the Upgraded turbine maps in the analytical model. From 70- to 90-percent gas generator speed the power increased by 1 to 1.2 percent for a 1-percent improvement in power turbine efficiency. At a gas generator speed below 70 percent, the power influence coefficient is greater, reaching almost 2 at 50-percent speed. The coefficient for SFC is shown in the upper half of figure 9 and amounts roughly to 0.8- to 1-percent reduction in SFC for each 1-percent improvement in power turbine efficiency.

Changing the power turbine efficiency does not significantly affect the compressor or compressor-drive turbine operating points. Pressure ratios and efficiencies of both the compressor and compressor-drive turbine were essentially unchanged. For a 1-percent improvement in power turbine efficiency, the power increased about 1 to 1.2 1.2 percent, which is smaller effect than that caused by changes to either the compressor or compressor-drive turbine efficiencies. The compressor efficiency affected power to about 2 percent, while the compressor-drive turbine affected power to about 1.8 percent. Therefore, of the three turbomachinery components, the engine performance was most sensitive to compressor efficiency and least sensitive to the power turbine efficiency. Changes in compressor-drive turbine and compressor efficiency affected the operating point of the other two machines. When the power turbine efficiency was changed, the effect on the compressor and compressor-drive operating points was insignificant.

Effect of Regenerator Effectiveness

The level of the regenerative effectiveness strongly affected engine SFC but had essentially no effect on engine power (fig. 10). The reference regenerator effectiveness was 0.876 for 80-percent gas generator speed. The reference effectiveness determined from the Lewis thermocouple test data was based on the calculated heat transferred to the low pressure side of the regenerator. Regenerator effectiveness varied from 0.867 to 0.928. The 0.928 effectiveness was the Chrysler goal at 80-percent gas generator speed. Figure 10 shows that power is not sensitive to regenerator effectiveness. Over the entire range of effectiveness covered, the power varied only 0.2 horsepower. However, the effect on SFC (fig. 10) is significant. The SFC decreased linearly as regenerator effectiveness was increased. The influence coefficients for power and SFC are plotted in figure 11 for 50- to 100-percent speed. The influence coefficient for power again shows insensitivity to regenerator effectiveness variations. The SFC influence coefficients, however, show a significant sensitivity to regenerator effectiveness; the sensitivity increased at lower speeds where the regenerator heat load was lighter. The SFC influence coefficient at the reference effectiveness (80-percent speed) was 1.75. A 1-percent increase in regenerator effectiveness would thus reduce the SFC by 1.75 percent. A 100-percent speed the SFC reduction would be slightly more than 1 percent; at 50-percent speed it would increase to a 4-percent improvement. To reiterate, a 1-percent improvement in regenerator effectiveness from the reference level of 0.876, accomplished for example by an increase in the size of the core matrix, would lower the SFC by 1.75 percent. At 50-percent gas generator speed the engine with that new regenerator would then provide an SFC advantage of 4 percent over the engine with the original regenerator.

Effect of Regenerator Pressure Drop

In the regenerator, which is a rotating matrix periodic-flow heat exchanger, the gas flows from both the high- and low-pressure sides and passes through the same rotating disk flow passages. On the low-pressure side the volumetric flow is highest and pressure drop highest. Figure 12 shows the sensitivity of output power and SFC to the regenerator pressure drop fraction at gas generator speeds from 50 to 100 percent. The normal pressure drop fractions for both the high- and low-pressure sides are listed for each speed in the figure. In figure 12 the reference normalized pressure ratio is located at the abscissa value of 1. The pressure drop fraction was varied from zero to three times the reference pressure drop fraction, except at 100 percent. As the pressure drop was varied, the ratio of high-side to low-side pressure drop was held at the same value as it was for the reference case. Regenerator pressure drop

affects engine power by reducing the pressure drop that can be taken across the power turbine. The influence coefficients for the power and SFC are shown in figure 13. From 60- to 95-percent gas generator speed the power increased about 0.16 percent for each 1-percent reduction of the pressure drop fraction. For the 60- to 95-percent speed the SFC was reduced by 0.13 percent for each 1-percent reduction in pressure drop fraction.

Sensitivity to Flow Leaks

Any flow leak tends to degrade engine performance. Flow leak paths and mass flow for each leak were estimated by Chrysler for the initial design. These estimates were made at 50-, 60-, 70-, 80-, 90-, 95-, and 100-percent gas generator speed. The exact bleeds and leakage paths were used as reference values for the analytical model. Sensitivity was investigated at only 60-, 80-, and 90-percent gas generator speeds. The block diagram of the engine components (fig. 1) shows the leakage paths. For the sensitivity check, each leakage flow was varied from zero to a value greater than Chrysler's estimate. Power decreased and SFC increased as flow leakage increased. The appendix lists tabulated influence coefficients at the three gas generator speeds where flow leak sensitivity was checked. The notation $4 \rightarrow 33$ indicates leakage from duct 4 to station 33 in figure 1. The leakage paths can be categorized as leaks from the high-pressure side that do not pass through either turbine, leaks that pass through one turbine but bypass the other, and leaks that pass through both turbines. Variation of engine power for a variation of bleed fraction from 0 to 0.01 is shown in figure 14 for all nine leakage paths. The bleed fraction is the ratio of flow leak to total flow at that location. The reference values for each leak are shown. Figure 14 shows the power variation to be linear with bleed fraction changes. Flow leaks bypassing both turbines exit from ducts 4, 5, 8, and 12. Leaks along these paths had the most significant effect, as noted from their steep slopes in figure 14. The leaks least affecting power were from ducts 6 and 7 of figure 1; since these leaks were to points upstream of both turbines, the leakage flow still passes through both turbines. The leakage flows from ducts 13 and 18 bypassed the compressor-drive turbine, while the leak from duct 30 bypassed the power turbine. The sensitivity to these flows was intermediate between the other two extremes. All nine leaks have a detrimental effect on SFC (fig. 15). The tabulation of the influence coefficients in the appendix shows that the flow leaks bypassing both turbines have about the same effect on power. At 80-percent gas generator speed the power influence coefficient was about 0.03 for leakage flows 4, 5, 8, and 12. These same flow leaks all affected SFC adversely but to differing degrees. Leak $5 \rightarrow 32$ had the greatest effect on SFC. This leak was from the regenerator inlet on the high-

pressure side to the regenerator inlet on the low-pressure side. The next most sensitive leak (4 → 33) was the leak across the regenerator disk seal from the regenerator high-pressure inlet side to the regenerator low-pressure discharge side.

Sensitivity to Heat Leaks

Heat leakage paths and the magnitude of each leak were also estimated by Chrysler at the initial design stage for gas generator speeds from 50 to 100 percent. The Chrysler estimates were used as reference values. Heat losses affected system performance in much the same way that regenerator effectiveness did; the engine power was practically unaffected, and the SFC was adversely affected. The heat losses are of two types, losses leaving the engine to the surrounding environment and heat transferred from engine hot sections back to cooler sections. In figure 16 the effects of the heat leaks are shown for 60-, 80-, and 90-percent gas generator speed. The component from which the heat is transferred is indicated by a number corresponding to a component in figure 1. The figure also shows the heat leakage paths. The reference heat flow is marked with a symbol on the line. The net heat flow for each component was used. In the case of heat leak 7 in figure 16 for 80-percent speed, the heat flow is a heat addition to the compressor discharge duct; this flow results from heat leaking back along three different paths and exceeds the heat loss from the diffuser scroll to ambient. Thus, at 80-percent speed and lower, there is a net heat input at 7. At 90-percent speed and above, the balance is such that there is a net heat loss from 7. Variations about the Chrysler reference magnitude were made for all five composite heat leaks, and the effect on SFC is shown in figure 16. The effects of heat transferred from 11, 15, and 22 were greatest, and the effect of 18 only slightly less as determined from the slopes. The SFC effect from variations to heat leak 7 were much less significant. The trends were consistent for all gas generator speeds. The heat leaks did not effect engine power except for one leak, 18, which appeared to cause an unexpected trend until the reasons for it were examined. First, it must be remembered that the scale on the ordinate of the power against heat flow plot is greatly expanded. The heat leak in question is a loss from the interturbine duct. The unanticipated trend of increased engine power with increased heat leak is due solely to the method of controlling temperature with the variable power turbine nozzle. The controlled temperature was the power turbine discharge temperature. In order to maintain a constant power turbine discharge temperature as the interturbine duct heat loss increased, burner outlet temperature had to increase. More fuel was required in the combustor to provide the higher peak cycle temperature. Thus, as heat losses from the interturbine duct increased, the

engine control method resulted in higher peak cycle temperature. Had the control method been different, for example, if the compressor-drive turbine inlet temperature had been controlled and had allowed the turbine discharge temperature to vary, the trend would have been just the opposite. The Chrysler method of controlling power-turbine discharge temperature was to keep the regenerator hot spot temperature below some prudent limit. Tabulated values for influence coefficients of the heat leaks considered are shown in the appendix.

Sensitivity to Shaft Parasitic Losses

Sensitivity of engine power to the parasitic losses of the gas generator shaft and to the power turbine shaft was considered by varying these losses independently from zero to the reference value shown in the appendix. Parasitic losses have a strong effect on both power and SFC. Reducing parasitic power results in an increase in engine power without any fuel rate increase or it results in a direct fuel saving for the same power. For the power turbine shaft a decrease of 1-kilowatt parasitic loss resulted in a 1-kilowatt increase in engine power. The influence coefficients for power and SFC are shown in figure 17. The magnitude of the influence coefficients indicates that the engine performance is more sensitive to power turbine parasitic losses than to gas generator shaft losses. The SFC changes reflect engine power changes with essentially no change in actual fuel consumption. For the same power, fuel consumption would be reduced.

Sensitivity to Compressor Inlet Temperature

The compressor inlet temperature has a significant effect on engine performance. For sensitivity calculations the power turbine discharge temperature and both shaft speeds were held constant as compressor inlet temperature variations were made. Reducing compressor inlet temperature resulted in a higher compressor pressure ratio and increased air mass flow. After the compressor drive turbine had rematched, its pressure ratio was slightly decreased but the turbine inlet temperature was higher. Since compressor pressure ratio was higher with a slightly lower compressor-drive turbine pressure ratio, it follows that the power turbine pressure ratio increased. This resulted in a 4.5-percent increase in engine power for a 1-percent decrease in compressor inlet temperature in the gas generator speed range from 70 to 90 percent. Below 70 percent and above 90 percent the magnitude of the influence coefficient for power and SFC were considerably higher. Again the analytical model predicted poor high-speed performance with high sensitivity to any operating condition improvement such as reduced compressor inlet temperature.

Sensitivity to Power Turbine Discharge Temperature

The power turbine discharge temperature is actively controlled by means of a variable turbine nozzle. The power turbine nozzle could have also been used to control the peak turbine inlet temperature of the compressor drive turbine, however, controlling the power turbine discharge temperature prevented excessive regenerator peak temperatures. Variations of power turbine discharge temperature (T_{20} of fig. 1) were made while compressor inlet temperature and both shaft speeds were held constant. As changes in T_{20} were made, the compressor-drive turbine inlet temperature followed in the same direction. The compressor operating point was essentially unchanged with only a slight decrease in pressure ratio. When power turbine discharge temperature was raised, the inlet temperature to the compressor-drive turbine increased and a lower drive turbine pressure ratio was sufficient to provide compressor work and thereby permit a higher power turbine pressure ratio. The influence coefficients for engine power and SFC are shown in figure 19. The change in power at 80-percent gas generator speed was 3.1 percent for a 1-percent increase in power turbine discharge temperature. At the other gas generator speeds the sensitivity was greater. The SFC reduction at the 80-percent speed point was about 2.2 percent. Again the high and low gas generator speed points showed extreme sensitivity to any parameter that would improve performance.

CONCLUDING REMARKS

A sensitivity study was conducted to obtain influence coefficients for a number of the most important component performance and operating parameters for the Upgraded engine 5-4. Engine 5-4 was on test at the NASA Lewis Research Center when a program was underway by Chrysler and the government to correct a power shortfall in the early development engines. Consequently, engine 5-4 was modelled analytically and the sensitivity study was performed with that model. The appendix is a complete tabulation of all influence coefficients. Some remarks and general observations about some of the trends are the following:

(1) Performance changes to the compressor or compressor-drive turbine affect the operating points of the other rotating machines. Improving the efficiency of the compressor shifted the operating point of both the compressor-drive turbine and power turbine. Changes of compressor-drive turbine efficiency affected the operating point of the compressor and the power turbine. Changes in the power turbine performance did not have a significant effect on the compressor and compressor-drive turbine operating points.

(2) The engine output is most sensitive to compressor inlet temperature, power turbine discharge temperature, and turbomachinery efficiencies. Variations in power turbine efficiency affected performance to a lesser degree than did compressor or compressor-drive efficiency.

(3) Regenerator effectiveness had little effect on engine power but a strong effect on fuel consumption.

(4) Regenerator pressure drop reduction resulted in an increase in power turbine pressure ratio, and this resulted in increased engine power. This same trend also holds for duct piping pressure losses.

(5) All mass flow leaks adversely affected power and specific fuel consumption. Flow leaks that bypassed both turbines were most serious. Flow leaks bypassing only one turbine were less serious.

(6) Heat leaks affected fuel consumption, but their effect on output power was insignificant.

(7) Engine power and specific fuel consumption were more sensitive to parasitic losses on the power turbine shaft than on the gas generator shaft.

APPENDIX - INFLUENCE COEFFICIENTS FOR CHRYSLER UPGRADED ENGINE

Tabulations of all of the calculated influence coefficients for gas generator speeds from 50 to 100 percent are included in this appendix.

The use of the influence coefficient is illustrated by the following example. To find the change in power if the compressor efficiency is improved from 0.741 to 0.75 at 80 percent gas generator speed, the influence coefficient for power from the 80 percent N_{GG} table. For this example it is 1.845:

$$\frac{\frac{\Delta H_p}{H_{p,\,ref}}}{\frac{\Delta \eta_c}{\eta_{c,\,ref}}} = \frac{\frac{\Delta Y}{Y}}{\frac{\Delta X}{X}} = 1.845$$

$$\Delta H_p = 1.845 \times H_{p,\,ref} \times \frac{\Delta \eta_c}{\eta_{c,\,ref}}$$

From the same table,

$$\eta_{c,\,ref} = 0.741$$

$$H_{p.\,ref} = 24.42 \text{ hp } (18.21 \text{ kW})$$

$$\Delta H_p = 1.845 \times 24.42 \times \frac{0.75 - 0.741}{0.741} = 0.547 \text{ hp}$$

The new power is

$$H_p = H_{p,\,ref} + \Delta H_p = 24.42 \text{ hp} + 0.55 \text{ hp} = 24.97 \text{ hp}$$

REFERENCES

1. Warren, E. L.: Lewis Support of Chrysler Upgraded Engine Program. Highway Vehicle Systems Contractor Coordinating Meeting, CONF-771037, Dept. of Energy, Mar. 1978, pp. 143-149.

2. Wong, R. Y.: In-House Test Program on Turbomachinery Components at NASA Lewis Research Center. Highway Vehicle Systems Contractor Coordinating Meeting, CONF-7805102, Dept. of Energy, Sep. 1978, pp. 83-92.

3. Roelke, R. J.; and McLallin, K. L.: Cold-Air Performance of the Compressor-Drive Turbine of the Department of Energy Baseline Automotive Gas-Turbine Engine. DOE/NASA/1011-78/25, NASA TM-78894, 1978.

4. Kofskey, M. G.; and McLallin, K. L.: Cold-Air Performance of Free-Power Turbine Designed for a 112 kW Automotive Gas-Turbine Engine. Part III: Effect of Stator Vane End Clearances on Performance. DOE/NASA/1011-78/29, NASA TM-78956, 1978.

5. Fishbach, L. H.; and Caddy, M. J.: NNEP - The Navy NASA Engine Program. NASA TM X-71857, 1975.

6. Schmidt, F. W.; and Wagner, C. E.: Baseline Gas Turbine Development Program. COO-2749-18, Dept. of Energy, 1977.

INFLUENCE COEFFICIENTS FOR CHRYSLER UPGRADED ENGINE

(a) Gas generator speed, N_{GG}, 50 percent, 29 250 rpm; power turbine speed, N_{pt}, 15 040 rpm

x	x_{std}	$\Delta x/x_{std}$	y																		Comments
			Power, kW (net)	Fuel, kg/hr	SFC, kg/kW-hr	PR_c	PR_{ct}	PR_{pt}	η_{cp}	η_{ct}	η_{pt}	η_{reg}	EFF_{net}	T_9, K	T_{11}, K	T_{15}, K	T_{19}, K	T_{20}, K	T_{23}, K	T_{26}, K	$\dot{\omega}_{al}$,
			y_{std}																		
			2.18	3.26	1.4948	1.4888	1.2785	1.1051	0.72560	0.74343	0.54460	0.92323	0.0557	358.7	964.4	1094.5	1034.4	1020.6	1011.6	431.1	0.1869	
			Influence coefficient, $(\Delta y/y_{std})/(\Delta x/x_{std})$																		
Efficiency																					
η_c	0.7256	0.011	2.46	-0.375	-2.649	0.066	-0.218	0.268	1.0	0.134	-0.676	0.018	2.741	-0.115	0.005	-0.005	0.024	0	0	-0.112	-0.281	Scaled
η_{ct}	.74343	.010	2.666	-.135	-2.483	.059	-.228	.299	.040	1.0	-.899	.016	2.446	.017	.011	.035	.026	↓	.005	-.013	-.283	turbine
η_{pt}	.5446	.008	1.345	0	-1.188	0	-.010	-.012	-.004	-.004	1.0	0	1.175	-.002	0	.013	.014		.007	0	.016	maps
η_c	.7096	.011	6.173	-.394	-6.156	.013	-.247	.219	1.0	.006	-.125	-.001	6.632	-.129	-.005	-.005	.035		0	-.133	.091	Upgraded
η_{ct}	.6651	.013	8.685	-.301	-8.083	.064	-.267	.338	.096	1.0	-.653	.007	8.973	.011	.004	.051	.050		0	-.355	-.192	maps
η_{pt}	.6731	.003	1.978	-1.149	-3.122	-.027	-.091	0	-.033	.286	1.0	-.004	3.712	-.006	0	0	.021		0	-.178	.100	
η_{reg}	.92323	.006	0	-4.048	-3.889	0	0	-.015	-.004	0	.083	1.0	4.064	-.003	.587	0	0		.009	-1.488	-.008	
Power losses, kW																					
A_{ct}	0.72	-0.01	-0.226	0.029	0.208	-0.004	0.018	-0.024	-0.002	-0.010	0.038	-0.001	-0.264	-0.001	-0.001	0	-0.003	0	0	0.001	0.021	
A_{pt}	.78	-1.0	-.357	0	.263	0	0	0	0	0	0	0	-.357	0	0	0	0	0	0	0	0	
Temperature, K																					
T_1	302.6	-0.01	17.361	-1.729	13.317	-0.608	-0.046	-0.559	-0.325	0.015	0.151	0.037	-15.25	0.800	0.046	-0.097	-0.092	0	0	0.517	-0.608	
T_{20}	1020.6	.01	10.609	.861	8.813	.150	-.168	.332	.255	-.206	-.085	.025	9.657	.023	.999	1.005	1.052	1.0	1.011	.278	-.405	
$(\Delta p/p)_{reg}$	----------	-0.5	-0.304	-0.026	0.242	0.001	0.001	-0.025	0	0	0.032	0	-0.272	0	0	-0.003	-0.003	0	0	-0.001	-0.004	

(b) Gas generator speed, N_{GG}, 60 percent, 35 100 rpm; power turbine speed, N_{pt}, 19 630 rpm

x	x_{std}	$\Delta x/x_{std}$	y																		Comments
			Power, kW (net)	Fuel, kg/hr	SFC, kg/kW-hr	PR_c	PR_{ct}	PR_{pt}	η_{cp}	η_{ct}	η_{pt}	η_{reg}	EFF_{net}	T_9, K	T_{11}, K	T_{15}, K	T_{19}, K	T_{20}, K	T_{23}, K	T_{26}, K	$\dot{\omega}_{a1}$, kg/sec	
			y_{std}																		
			5.53	4.89	0.8839	1.7709	1.4177	1.1693	0.72997	0.74330	0.60379	0.90803	0.0942	379.7	958.2	1124.6	1044.6	1020.6	1013.2	460.4	0.2432	
			Influence coefficient, $(\Delta y/y_{std})/(\Delta x/x_{std})$																		
Efficiency																					
η_c	0.72997	0.012	1.852	-0.319	-2.145	0.082	-0.357	0.426	1.000	0.223	-0.883	0.020	2.188	-0.161	0.010	-0.008	0.041	0	0	-0.140	-0.258	Scaled turbine maps
η_{ct}	.74330	.011	1.910	0	-1.902	.080	-.350	.455	.085	1.0	-1.023	.018	1.881	.012	.010	.044	.042	↓	↓	-.007	-.254	
η_{pt}	.60379	.008	1.212	.119	-1.070	0	-.009	0	-.002	-.005	1.0	0	.955	-.002	0.	.019	.020			.003	.010	
η_c	.7238	.011	2.763	-.110	-2.782	.021	-.338	.306	1.0	.003	-.042	-.001	2.847	-.182	-.005	-.009	.044			-.130	-.059	Upgraded maps
η_{ct}	.7092	.013	2.980	.085	-2.776	.088	-.363	.487	.093	1.0	-.988	.011	2.845	.015	.009	.057	.053			.003	-.238	
η_{pt}	.6498	.002	1.602	.237	-1.328	-.059	-.179	.045	-.043	.349	1.0	0	1.229	-.015	0	.026	0.			.037	.132	
η_{reg}	.90803	.007	-.182	-3.124	-2.985	0	0	-.023	-.006	0	.078	1	3.003	0	.570	0	0			-1.318	-.003	
Power losses, kW																					
A_{ct}	1.03	-0.01	-0.113	0.025	0.124	-0.004	0.023	-0.031	-0.006	-0.003	0.067	-0.001	-0.142	-0.001	-0.001	0.001	-0.003	0	0	0.001	0.017	
A_{pt}	1.16	-1.0	-.210	0	.174	0	0	0	0	0	0	0	-.210	0	0	0	0	0	0	0	0	
Flow leaks, ω_{leak}/ω																					
4 → 33	(a)	-1.0	-0.036	-0.001	0.034	-0.003	0.004	-0.007	-0.004	-0.002	0.013	0	-0.036	0	0	0	-0.001	0	0	-0.002	0.010	
5 → 32	↓	↓	-.037	.029	.064	-.003	.003	-.007	-.004	-.002	.013	0	-.069	↓	-.006	0	-.001	↓	-.006	.011	.010	
6 → 27			.003	.028	.026	0	0	0	0	0	-.001	.001	-.026		0	.006	0		0	.012	0	
7 → 28			.002	.028	.027	0	0	0	0	0	0	.001	-.027		0	0	0		0	.012	0	
12 → 31			-.039	.005	.042	-.003	.004	-.007	-.004	-.002	.014	-.001	-.044		-.001	0	-.001		-.001	0	.010	
13 → 29			-.020	.007	.026	-.003	.003	-.007	-.003	-.002	.017	-.001	-.027		0	.001	-.001		0	0	.010	
18 → 30			-.018	-.002	.015	0	0	0	0	0	-.004	0	-.015		↓	0	0		↓	0	0	
30 → 38			-.008	.034	.042	-.002	.002	-.004	-.002	-.002	.011	0	-.044			.006	0			.013	.007	
8 → 34	↓	↓	-.038	-.001	.036	-.003	.003	-.007	-.004	-.002	.013	0	-.037	↓	↓	0	-.001	↓	↓	0	.010	
Heat loss duct																					
7	(b)	2	0	-0.003	-0.003	0	0	0	0	0	0	0	0.003	0.019	0.001	0	0	0	0	0.013	0	
11	↓	1	-.002	-.035	-.033	0	0	0	0	↓	.001	0	.034	0	0	0	↓	↓	↓	-.001	0	
15			-.001	-.034	-.033	0	0	0	0		0	↓	.034	↓	0	-.005				-.001	0	
18			-.011	-.032	-.021	-.001	.002	-.003	-.001		.008		.023		0	-.006				0	.003	
22	↓	↓	-.002	-.031	-.029	0	0	0	0	↓	0	↓	.031	↓	.006	0	↓	↓	.006	.001	0	
Temperature, K																					
T_1	392.6	-0.01	-6.258	-1.600	4.382	-0.745	0	-0.728	-0.268	0.017	1.157	0.046	-4.527	0.770	0.052	-0.089	-0.085	0	0	0.475	-0.705	
T_{20}	1020.6	.01	3.819	.727	-2.980	.171	-.243	.421	.189	-.186	-.669	.029	3.099	.026	.992	.986	1.045	1.0	1.009	.309	-.431	
$(\Delta p/p)_{reg}$	--------	-0.5	-0.178	-0.024	0.142	0.001	0.002	-0.031	0.001	0	0.049	0	-0.152	0	0	-0.003	-0.003	0	0	-0.001	-0.003	

[a] Values may be obtained from fig. 14.
[b] Values may be obtained from fig. 15.

(c) Gas generator speed, N_{GG}, 70 percent, 40 950 rpm; power turbine speed, N_{pt}, 24 125 rpm

x	x_{std}	$\Delta x/x_{std}$	y: Power, kW (net)	Fuel, kg/hr	SFC, kg/kW-hr	PR_c	PR_{ct}	PR_{pt}	η_{cp}	η_{ct}	η_{pt}	η_{reg}	EFF_{net}	T_9, K	T_{11}, K	T_{15}, K	T_{19}, K	T_{20}, K	T_{23}, K	T_{26}, K	$\dot{\omega}_{al}$, kg/sec	Comments
			y_{std}: 10.54	7.16	0.6792	2.1341	1.5875	1.2403	0.73896	0.73785	0.63080	0.89329	0.1225	403.3	951.9	1157.0	1055.1	1020.6	1013.6	491.2	0.3057	
			Influence coefficient, $(\Delta y/y_{std})/(\Delta x/x_{std})$																			
Efficiency																						
η_c	0.73896	0.0115	1.776	-0.227	-1.936	0.067	-0.475	0.499	1.000	0.148	-0.624	0.015	1.977	-0.217	0	-0.017	0.052	0	0	-0.170	-0.156	Scaled turbine maps
η_{ct}	.73785	.0104	1.970	.122	-1.790	.068	-.484	.596	.049	1.0	-.854	.014	1.882	.012	.011	.060	.061			-.001	-.170	
η_{pt}	.6308	.007	1.166	.174	-.997	0	-.017	0	0	-.002	1.0	0	1.010	0	0	.026	.029			.002	.002	
η_c	.7373	.011	2.056	-.122	-2.128	.034	-.420	.378	1.0	-.015	.083	-.001	2.172	-.229	-.011	-.018	.063			-.162	-.096	Upgraded maps
η_{ct}	.7365	.016	1.959	.133	-1.767	.069	-.480	.591	.053	1.0	-.881	.009	1.777	.010	.004	.055	.060			.003	-.167	
η_{pt}	.6191	.006	1.163	.180	-.966	-.008	-.045	-.014	-.005	.075	1.0	0	.905	-.002	0	.026	.038			.002	.024	
η_{reg}	.89329	.009	-.082	-2.425	-2.275	0	.007	-.037	-.005	-.002	.051	1.0	2.368	0	.548	0	-.006			-1.169	0	
Power losses, kW																						
A_{ct}	1.40	-0.01	-0.090	0.017	0.095	-0.003	0.023	-0.029	-0.002	-0.008	0.042	-0.001	-0.105	0.001	0	0.001	-0.003	0	0	0	0.008	
A_{pt}	1.57	-1.0	-.150	0	.131	0	0	0	0	0	0	0	-.151	0	0	0	0	0	0	0	0	
Temperature, K																						
T_1	302.6	-0.01	-4.676	-1.632	2.910	-0.859	0.044	-0.874	-0.168	0.001	0.865	0.063	-2.967	0.731	0.064	-0.096	-0.105	0	0	0.429	-0.794	
T_{20}	1020.6	.01	2.725	.664	-2.007	.179	-.403	.607	.146	-.010	-1.016	.035	2.036	.028	.987	.962	1.054	1.0	1.003	.320	-.435	
$(\Delta p/p)_{reg}$	----------	-0.5	-0.164	-0.026	0.127	0.001	0.003	-0.038	0.001	0	0.033	0	-0.136	0	0	-0.004	-0.005	0	0	-0.001	-0.002	

(d) Gas generator speed, N_{GG}, 80 percent, 46 800 rpm; power turbine speed, N_{pt}, 30 800 rpm

x	x_{std}	$\Delta x/x_{std}$	y: Power, kW (net)	Fuel, kg/hr	SFC, kg/kW-hr	PR_c	PR_{ct}	PR_{pt}	η_{cp}	η_{ct}	η_{pt}	η_{reg}	EFF_{net}	T_9, K	T_{11}, K	T_{15}, K	T_{19}, K	T_{20}, K	T_{23}, K	T_{26}, K	$\dot{\omega}_{al}$, kg/sec	Comments
			y_{std}: 18.21	10.38	0.570	2.6065	1.7838	1.3230	0.741	0.74538	0.66124	0.87643	0.1460	431.2	945.9	1194.8	1067.7	1020.6	1014.3	526.2	0.3799	
			Influence coefficient, $(\Delta y/y_{std})/(\Delta x/x_{std})$																			
Efficiency																						
η_c	0.741	0.01	1.845	-0.131	-1.944	0.038	-0.595	-0.696	1.0	0.075	-0.730	0.009	1.989	-0.277	-0.012	-0.019	0.073	0	0	-0.199	-0.088	Scaled turbine maps
η_{ct}	.745	↓	2.006	.219	-1.740	.058	-.644	.764	.034	1.0	-.813	.013	1.780	.009	.006	.079	.083	↓	.005	-.002	-.129	
η_{pt}	.658		1.197	.212	-1.014	.004	-.027	.015	.003	-.001	1	.001	1.001	.001	0	.041	.051		.005	.003	-.008	
η_c	.741		1.914	-.144	-2.019	.046	-.699	.750	1.0	.152	-.868	.009	2.063	-.277	-.006	-.019	.078		0	-.198	-.099	Upgraded maps
η_{ct}	.745		1.881	.201	-1.653	.058	-.638	.764	.035	1.0	-.885	.013	1.644	.009	.006	.060	.078		0	0	-.129	
η_{pt}	.658		1.156	.194	-.961	0	-.106	0	0	.122	1.0	.002	1.017	0	0	.039	.044		0	-.002	.008	
η_{reg}	.87643	↓	-.123	-1.879	-1.754	-.004	.006	-.038	-.003	-.001	.027	1	1.779	0	.517	0	0	↓	.005	-1.006	.007	
Power losses, kW																						
A_{ct}	1.83	-1.0	-0.070	0.008	0.073	-0.002	0.023	-0.027	-0.001	-0.003	0.027	0	-0.079	0	0	0.001	-0.003	0	0	0	0.004	
A_{pt}	2.27	-1.0	-.126	0	.112	0	0	0	0	0	0	0	-.126	0	0	0	0	0	0	0	0	
Flow leaks, ω_{leak}/ω																						
4 → 33	(a)	-1.0	-0.029	-0.003	0.026	-0.003	0.005	-0.009	-0.002	-0.001	0.025	0	-0.026	-0.001	0	0	-0.051	0	0	-0.002	0.008	
5 → 32	↓	↓	-.030	.015	.044	-.003	.005	-.009	-.002	.001	.008	0	-.046	-.001	-.005	0	-.001	↓	-.005	.007	.008	
6 → 27			.002	.017	.015	0	0	.001	0	0	-.001	.001	.015	0	0	.006	0		0	.009	0	
7 → 28			-.001	.017	.016	0	0	0	0	0	0	.001	-.016	0	.001	0	0		0	.009	0	
12 → 31			-.031	.001	.031	-.003	.005	-.009	-.002	-.001	.009	-.001	-.033	-.001	-.001	0	-.001		-.001	0	.008	
13 → 29			-.014	.004	.018	-.003	.005	-.009	-.002	-.001	.013	-.001	-.019	-.001	0	.001	-.001		0	0	.007	
18 → 30			-.017	-.002	.014	0	0	0	0	0	-.005	0	-.015	0	0	0	0		↓	0	0	
30 → 38			-.006	.021	.027	-.002	.002	-.006	-.001	-.001	.008	0	-.027	0	0	.005	0			.009	.006	
8 → 34	↓	↓	-.031	-.003	.027	-.003	.005	-.009	-.002	-.001	.009	0	-.028	-.001	0	0	-.001	↓	↓	0	.008	
Heat loss duct																						
7	(b)	2	0.001	-0.003	-0.003	0	0	0	0	0	0	0	0.003	0.016	0.001	0.	0	0	0	0.011	0	
11	↓	1	-.001	-.024	-.023	0	0	0	0	↓	0	↓	.023	0	0	0	↓	↓	↓	0	0	
15		↓	0	-.023	-.023	0	0	0	0		0		.023	↓	0	-.004				0	0	
18			-.009	-.023	-.014	-.001	.003	-.004	-.001		.005		.015	0	0	-.005			↓	0	.002	
22	↓	↓	-.001	-.020	-.019	0	0	0	0	↓	0	↓	.019	↓	.006	0	↓	↓	.006	.002	0	
Temperature, K																						
T_1	302.6	-0.01	-4.521	-1.884	2.544	-1.043	0.061	-1.068	-0.131	-0.008	0.775	0.095	-2.406	0.667	0.088	-0.126	-0.182	0	0	0.348	-0.966	
T_{20}	1020.0	.01	3.064	.779	-2.238	.184	-.676	.910	.112	.222	-1.060	.041	2.063	.031	.975	.977	1.083	1.0	1.008	.337	-.425	
$(\Delta p/p)_{reg}$	----------	-0.5	-0.162	-0.028	0.124	0.001	0.004	-0.048	0	0	0.026	0	-0.131	0	0	-0.005	-0.006	0	0	-0.001	-0.001	

[a] Values may be obtained from fig. 14.

[b] Values may be obtained from fig. 15.

(e) Gas generator speed, N_{GG}, 90 percent, 52 650 rpm; power turbine speed, N_{pt}, 33 640 rpm

x	x_{std}	$\Delta x/x_{std}$	y																	Comments
			Power, kW (net)	Fuel, kg/hr	SFC, kg/kW-hr	PR_c	PR_{ct}	PR_{pt}	η_{cp}	η_{ct}	η_{pt}	η_{reg}	EFF_{net}	T_9, K	T_{11}, K	T_{15}, K	T_{19}, K	T_{20}, K	T_{23}, K	T_{26}, K	$\dot{\omega}_{al}$, kg/sec	
			y_{std}																			
			30.34	15.08	0.4970	3.2436	2.0363	1.4097	0.73766	0.75272	0.69524	0.85651	0.1674	464.9	939.1	1238.8	1081.4	1020.6	1014.3	566.7	0.4718	
			Influence coefficient, $(\Delta y/y_{std})/(\Delta x/x_{std})$																			
Efficiency																						
η_c	0.73766	0.011	1.669	-0.168	-1.776	0.023	-0.745	0.851	1.0	0.058	-0.818	0.011	1.834	-0.335	-0.017	-0.029	0.091	0	0	-0.228	-0.080	Scaled turbine maps
η_{ct}	.75272	.009	1.989	.288	-1.616	.039	-.821	.997	.022	1.0	-.962	.010	1.654	.008	.006	.091	.104	↓	↓	.010	-.082	
η_{pt}	.69524	.007	1.149	.213	-.901	.009	-.035	0	.004	-.002	1.0	.003	.930	.003	.008	.051	.058			0	0	
η_c	.7381	.011	1.759	-.150	-1.867	.042	-.711	.566	1.0	.011	-.050	-.001	1.944	-.329	-.022	-.029	.089		↓	-.215	-.105	Upgraded maps
η_{ct}	.7401	.015	2.277	.374	-1.837	.018	-.851	.983	.011	1.0	-.813	-.002	1.911	.002	0	.096	.114		.004	.013	-.050	
η_{pt}	.6921	.005	1.014	.165	-.844	.019	-.116	-.043	.008	.108	1.0	.005	.879	.005	0	.045	.052		0	.020	0	
η_{reg}	.85651	.012	-.190	-1.474	-1.252	-.005	.017	-.079	-.003	-.001	.053	1.0	1.284	0	.483	-.008	-.008	↓	0	-.852	.008	
Power losses, kW																						
A_{ct}	2.32	-0.01	-0.059	0.004	0.060	-0.001	0.023	-0.027	-0.001	-0.002	0.021	0	-0.064	0	0	0	-0.003	0	0	0	0.001	
A_{pt}	2.81	-1.0	-0.094	0	.086	0	0	0	0	0	0	0	-.094	0	0	0	0	0	0	0	0	
Flow leaks, ω_{leak}/ω																						
4 → 33	(a)	-1.0	-0.032	-0.006	0.025	-0.005	0.006	-0.011	-0.002	0	0.008	0	-0.025	-0.001	0	0	-0.001	0	0	-0.003	0.006	
5 → 32	↓	↓	-.033	.008	.039	-.005	.006	-.012	-.002	↓	.008	0	-.041	-.001	-.005	0	-.001	↓	-.005	.005	.006	
6 → 27			.002	.013	.011	0	0	.001	0		0.	.001	-.011	0	.001	.006	0		0	.008	0	
7 → 28			.001	.013	.012	0	0	0	0		0	.001	-.012	0	.001	0.	0		0	.008	0	
12 → 31			-.034	-.002	.030	-.005	.006	-.012	-.002		.008	-.001	-.032	-.001	-.001	0	-.001		-.001	0	.006	
13 → 29			-.018	.001	.018	-.005	.005	-.012	-.002	-.001	.012	-.001	-.019	-.001	0	.001	-.001		0	0	.005	
18 → 30			-.016	-.003	.013	0	0	0	0	0	-.004	0	-.013	0	.001	0	0		.001	0	0	
30 → 38			-.010	.014	.024	-.004	.003	-.008	-.002	-.001	.008	.001	-.024	-.001	0	.005	-.001		0	.008	.004	
8 → 34	↓	↓	-.034	-.006	.027	-.005	.006	-.012	-.002	0	.009	0	-.027	.001	0	0	-.001	↓	0	-.001	.006	
Heat loss duct																						
7	(b)	2	-0.001	-0.003	-0.003	0	0	0	0	0	0	0	0.003	0.015	0.001	0	0	0	0	0.010	0	
11	↓	↓	-.001	-.020	-.019	0	0	0	0	↓	0	↓	.020	0	0	0	0	↓	↓	0	0	
15			0	-.019	-.019	0	0	0	0		0		.019	↓	0	-.005	0			0	0	
18			-.009	-.020	-.011	-.001	.003	-.005	-.001		.005		.011		0	-.005	-.001			0	.002	
22	↓	↓	-.001	-.017	-.015	0	0	0	0	↓	0	↓	.016	↓	.006	0	0	↓	.006	.002	0	
Temperature, K																						
T_1	302.6	-0.01	-4.455	-1.877	2.463	-1.055	0.159	-1.174	-0.043	-0.002	0.531	0.112	-2.564	0.639	0.095	-0.135	-0.160	0	0	0.314	-0.981	
T_{20}	1020.6	.01	3.455	1.032	-2.336	.231	-.759	1.030	.106	.035	-.709	.030	2.441	.043	.958	.980	1.118	1.0	1.008	.382	-.270	
$(\Delta p/p)_{reg}$	----------	-0.5	-0.156	-0.029	0.117	0	0.006	-0.060	0	0	0.027	0	-0.124	0	0	-0.007	-0.008	0	0	-0.001	0	

[a] Values may be obtained from fig. 14.
[b] Values may be obtained from fig. 15.

(f) Gas generator speed, N_{GG}, 95 percent 55 575 rpm; power turbine speed, N_{pt}, 33 650 rpm

x	x_{std}	$\Delta x/x_{std}$	y: Power, kW (net)	Fuel, kg/hr	SFC, kg/kW-hr	PR_c	PR_{ct}	PR_{pt}	η_{cp}	η_{ct}	η_{pt}	η_{reg}	EFF_{net}	T_9, K	T_{11}, K	T_{15}, K	T_{19}, K	T_{20}, K	T_{23}, K	T_{26}, K	$\dot{\omega}_{a1}$, kg/sec	Comments
			y_{std}																			
			33.82	16.98	0.5020	3.5111	2.1789	1.4061	0.71786	0.75746	0.71775	0.85036	0.1658	482.0	938.8	1255.8	1083.0	1020.6	1015.0	584.4	0.5082	
			Influence coefficient, $(\Delta y/y_{std})/(\Delta x/x_{std})$																			
Efficiency																						
η_c	0.71786	0.010	1.847	-0.182	-1.983	-0.028	-0.863	0.956	1.0	0.059	-0.951	0.011	1.997	-0.375	-0.017	-0.034	0.100	0	0	-0.259	-0.078	Scaled turbine maps
η_{ct}	.75746	.009	2.232	.342	-1.833	.006	-.929	1.121	-.006	1.0	-1.167	.008	1.863	.005	.006	.104	.120	↓	↓	0	-.067	
η_{pt}	.71775	.007	1.135	.111	-.978	.016	-.045	0	.010	0	1.0	0	1.007	.002	0	.055	.057			-.013	0	
η_c	.7194	.011	2.675	-.084	-2.680	.044	-.863	.735	1.0	.048	-.048	0	2.734	-.350	-.027	-.012	.123			-.235	-.106	Upgraded maps
η_{ct}	.7232	.019	4.022	.589	-3.186	.020	-1.020	1.262	.010	1.0	-.627	0	3.366	.004	0	.151	.178			.015	-.046	
η_{pt}	.7129	.005	.923	.143	-.780	.026	-.097	-.069	.026	.069	1.0	.002	.790	0.	0	.033	.038			0	0	
η_{reg}	.85036	.012	-.200	-1.344	-1.139	-.005	.019	-.082	-.005	-.001	.070	1.0	1.144	0	.469	-.004	-.008	↓	↓	-.792	0	
Power losses, kW																						
A_{ct}	2.59	-0.01	-0.060	0.005	0.060	0	0.023	-0.021	-0.001	-0.003	0.024	0	-0.061	0	0	0	-0.005	0	0	0	0	
A_{pt}	2.81	-1.0	-.084	0	.078	0	0	0	0	0	0	0	-.084	0	0	0	0	0	0	0	0	
Temperature, K																						
T_1	302.6	-0.01	-5.255	-1.936	3.152	-1.067	0.100	-1.132	0.128	-0.025	0.222	0.093	-3.199	0.568	0.089	-0.165	-0.181	0	0	0.285	-0.983	
T_{20}	1020.6	.01	7.299	1.591	-5.322	.324	-1.258	1.808	.234	.350	-.498	.019	5.619	.027	.941	1.088	1.269	1.0	1.002	.380	-.197	
$(\Delta p/p)_{reg}$	----------	-0.5	-0.165	-0.030	0.125	0	0.006	-0.067	0	0	0.037	0	-0.133	0	0	-0.007	-0.009	0	0	-0.001	0	

(g) Gas generator speed, N_{GG}, 100 percent, 58 500 rpm; power turbine speed, N_{pt}, 33 650 rpm

x	x_{std}	$\Delta x/x_{std}$	y: Power, kW (net)	Fuel, kg/hr	SFC, kg/kW-hr	PR_c	PR_{ct}	PR_{pt}	η_{cp}	η_{ct}	η_{pt}	η_{reg}	EFF_{net}	T_9, K	T_{11}, K	T_{15}, K	T_{19}, K	T_{20}, K	T_{23}, K	T_{26}, K	$\dot{\omega}_{a1}$, kg/sec	Comments
			y_{std}																			
			32.87	18.62	0.5665	3.7687	2.3952	1.3421	0.68534	0.75432	0.75953	0.84435	0.1469	502.7	938.8	1268.8	1077.6	1020.6	1015.2	604.2	0.5415	
			Influence coefficient, $(\Delta y/y_{std})/(\Delta x/x_{std})$																			
Efficiency																						
η_{cp}	0.68534	0.009	4.400	0.106	-4.153	-0.093	-1.478	1.689	1.0	0.449	-1.437	0.017	4.302	-0.424	-0.026	0.043	0.225	0	0	-0.291	-0.128	Scaled turbine maps
η_{ct}	.75432	.013	3.607	.524	-2.936	-.012	-1.078	1.345	-.038	1.0	-1.101	.007	3.085	.010	.005	.151	.178	↓	0	.007	-.058	
η_{pt}	.75953	.007	1.263	.209	-1.058	.023	-.066	.032	.027	.008	1.0	.002	1.069	-.003	0	.050	.066		0	0	.012	
η_{reg}	.84435	.013	-.359	-1.254	-.910	-.006	.030	-.112	-.007	-.006	.072	1.0	.917	0	.445	-.010	-.012	↓	.004	-.728	.007	
Power losses, kW																						
A_{ct}	2.85	-0.01	-0.153	-0.010	0.148	0	0.038	-0.045	-0.001	-0.012	0.032	0	-0.138	0	0	-0.004	-0.005	0	0	0	0	
A_{pt}	2.81	-1.0	-.087	0	-.080	0	0	0	0	0	0	0	.087	0	0	0	0	0	0	0	0	
$(\Delta p/p)_{reg}$	-------	-0.5	-0.256	-0.041	0.191	0.001	0.014	-0.084	-0.001	-0.003	0.040	0	-0.210	0	0	-0.010	-0.012	0	0	-0.001	0	

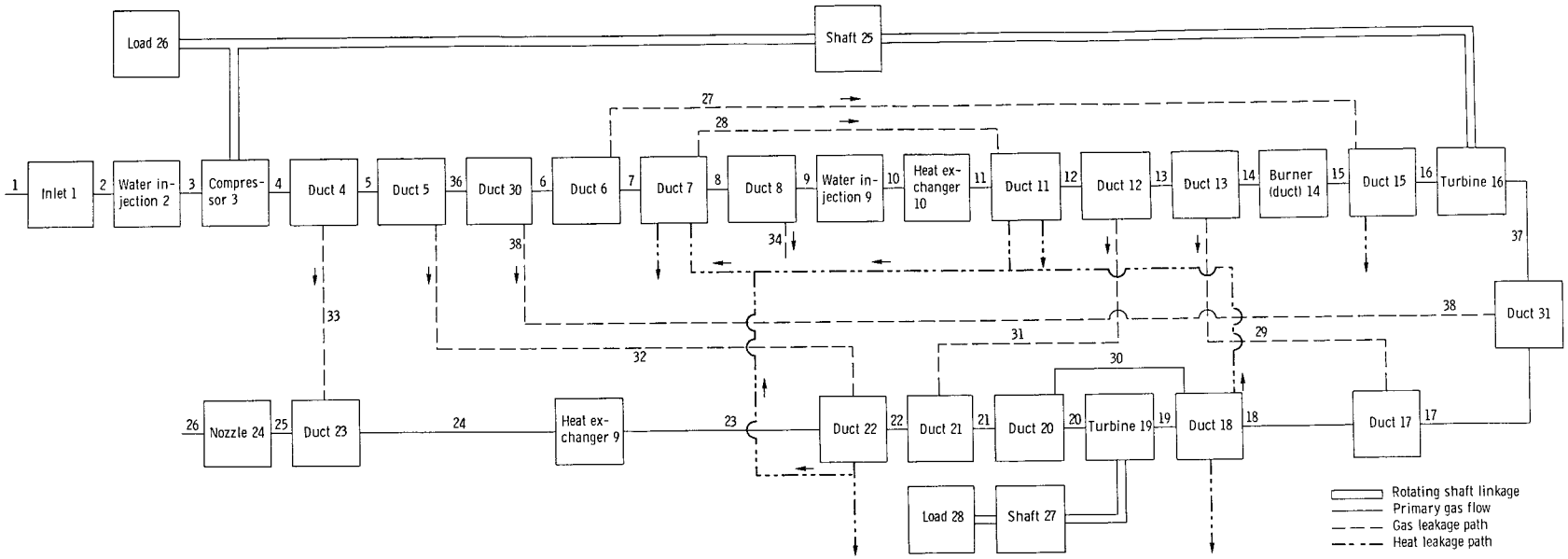

Figure 1. - Block diagram for Chrysler upgraded engine for use with Navy-NASA Engine Program computer code.

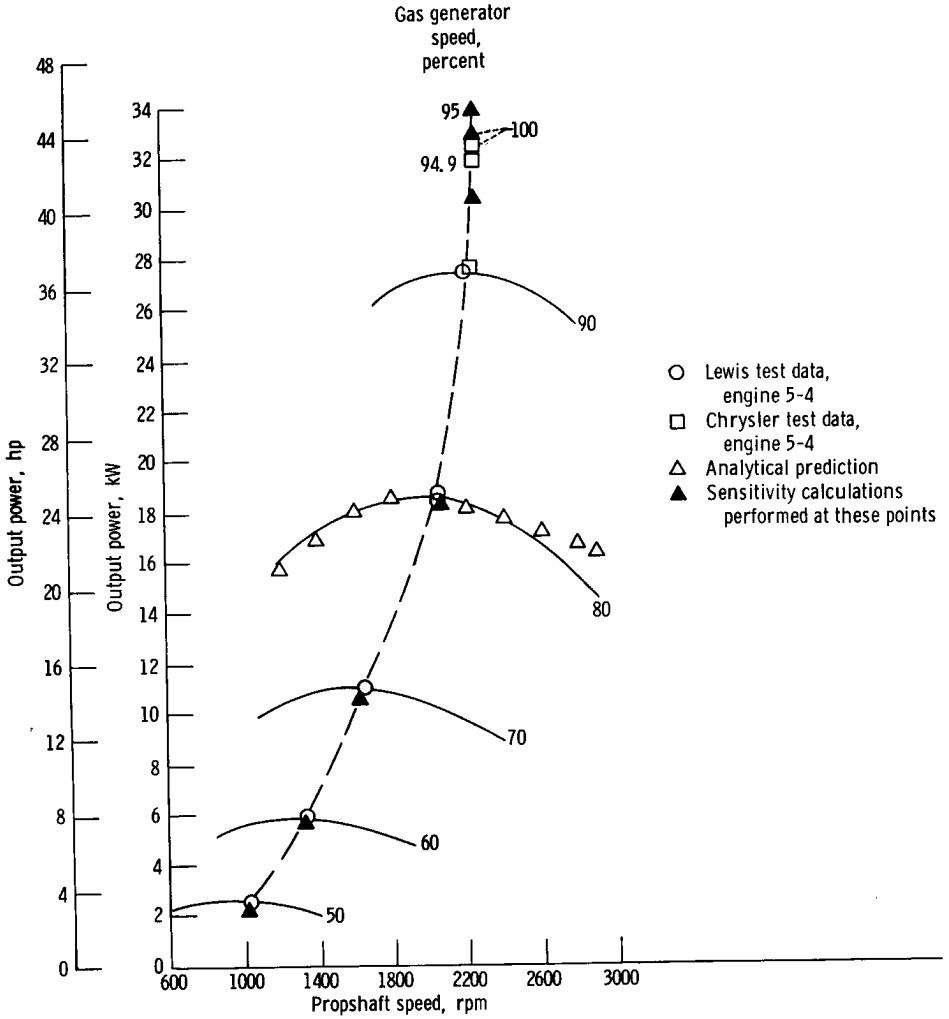

Figure 2. - Engine map showing correlation between engine test data and predicted performance.

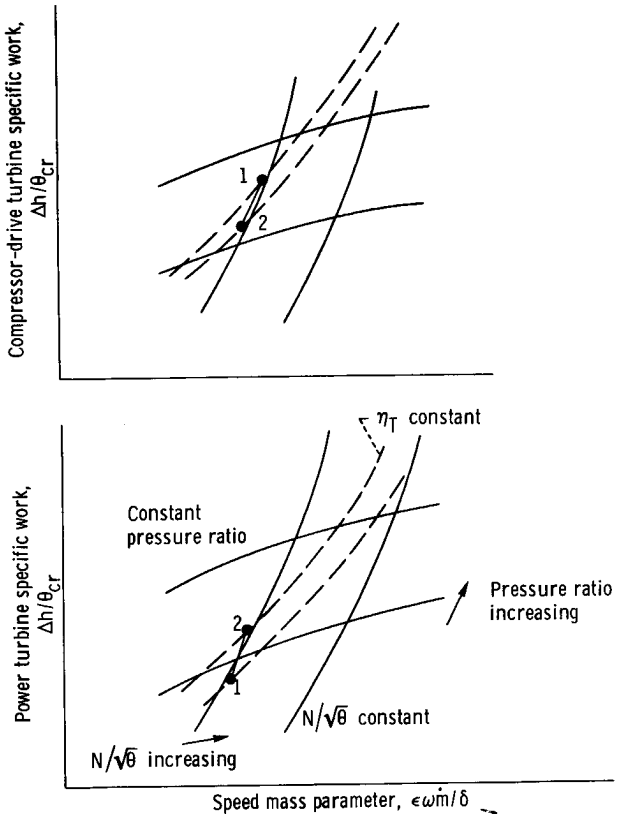

Figure 3. - Turbine maps showing shift of operating points when compressor efficiency is improved. Constant power turbine discharge temperature.

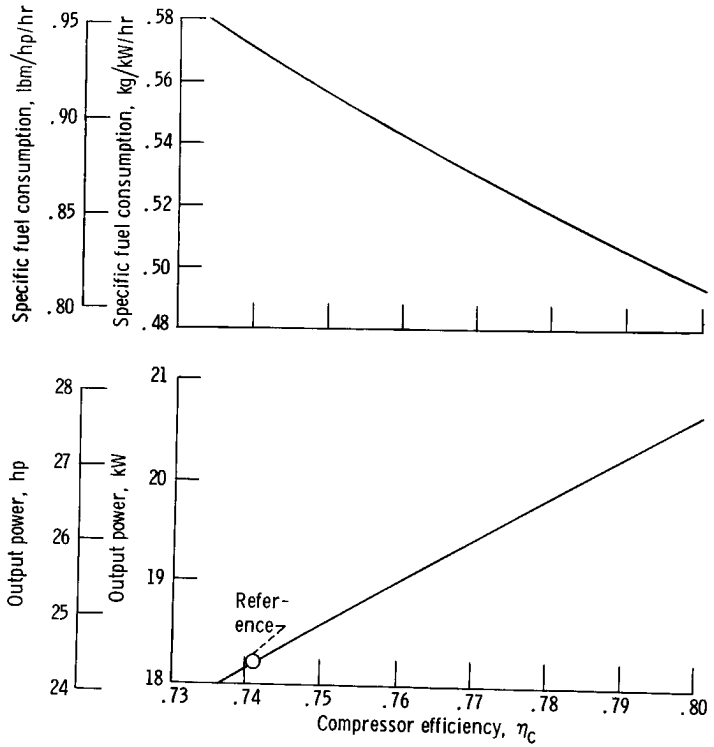

Figure 4. - Effect of compressor efficiency on power and specific fuel consumption. Gas generator speed, 46 800 rpm, 80 percent; power turbine speed, 30 030 rpm; power turbine discharge temperature, 1021 K (1837° R).

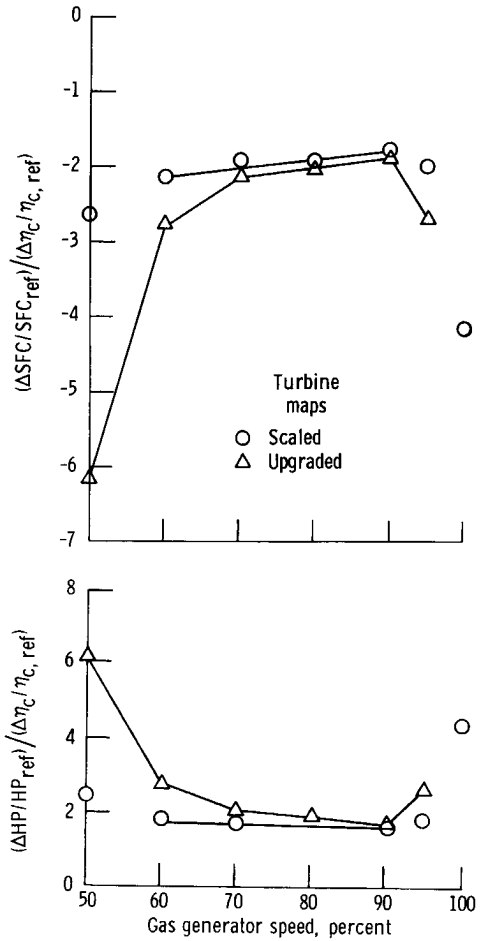

Figure 5. - Power and specific fuel consumption influence coefficients for improved compressor efficiency.

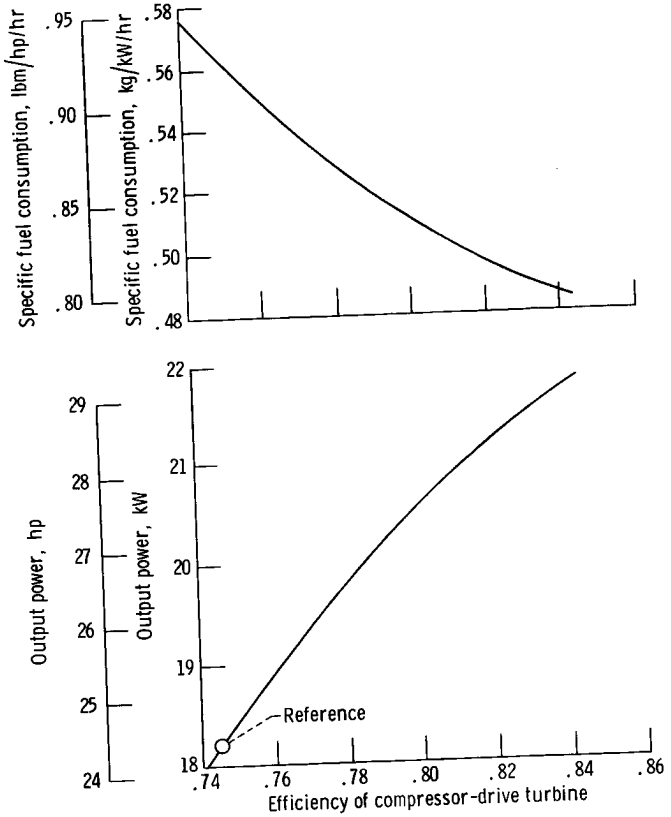

Figure 6. - Effect of compressor-drive turbine efficiency on power and specific fuel consumption. Gas generator speed, 46 800 rpm, 80 percent; power turbine speed, 30 030 rpm; power turbine discharge temperature, 1021 K (1837^{0} R).

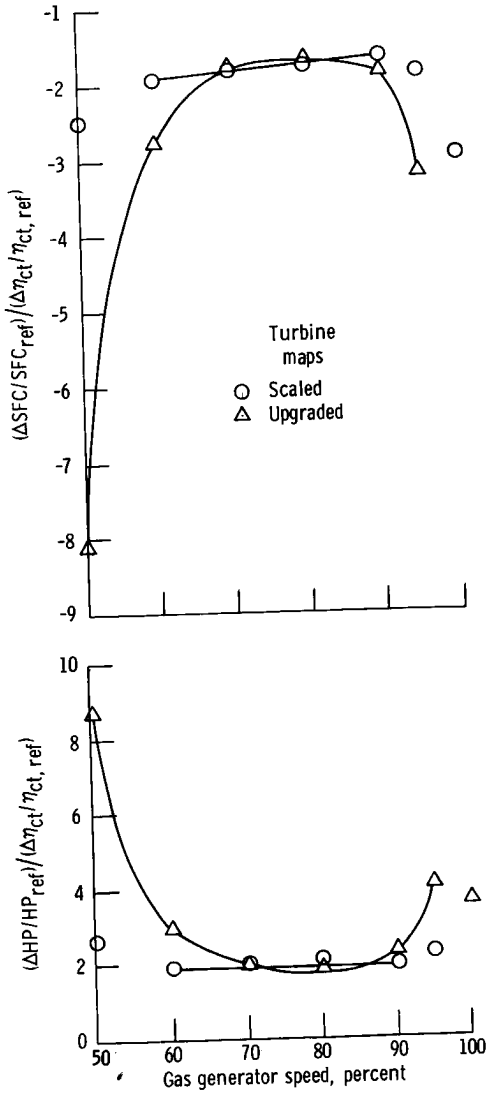

Figure 7. - Power and specific fuel consumption influence coefficients for improved compressor-drive turbine efficiency.

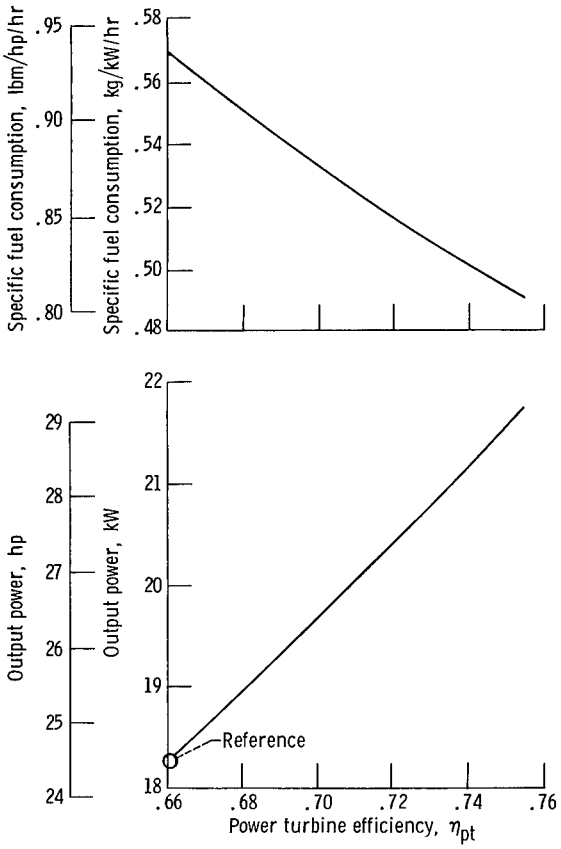

Figure 8. - Effect of power turbine efficiency on power and specific fuel consumption. Gas generator speed, 46 800 rpm, 80 percent; power turbine speed, 30 030 rpm; power turbine discharge temperature, 1021 K (1837° R).

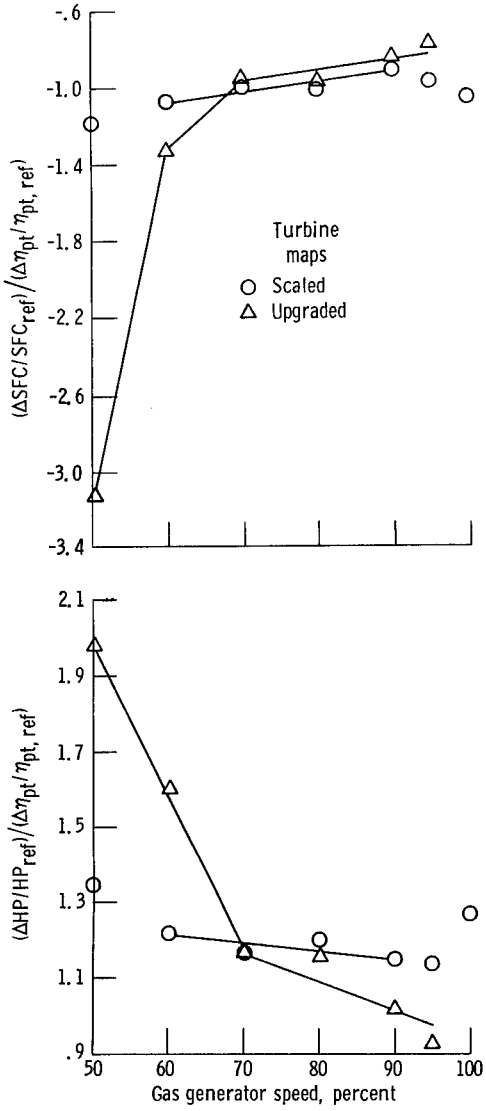

Figure 9. - Power and specific fuel consumption influence coefficients for improved power turbine efficiency.

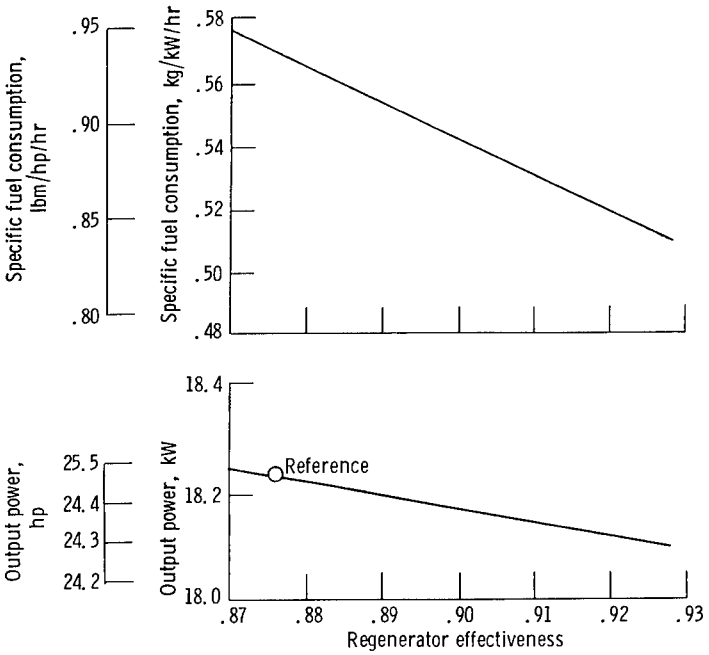

Figure 10. - Effect of regenerator effectiveness on power and specific fuel consumption. Gas generator speed, 46 800 rpm, 80 percent; power turbine speed, 30 030 rpm; power turbine discharge temperature, 1021 K (1837^0 R).

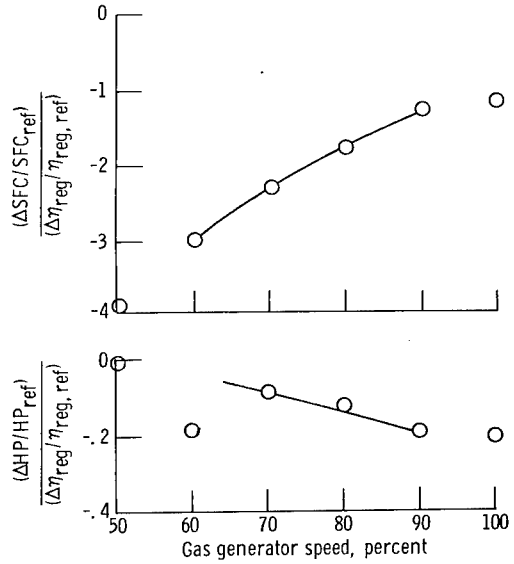

Figure 11. - Power and specific fuel consumption influence coefficients for improved regenerator effectiveness.

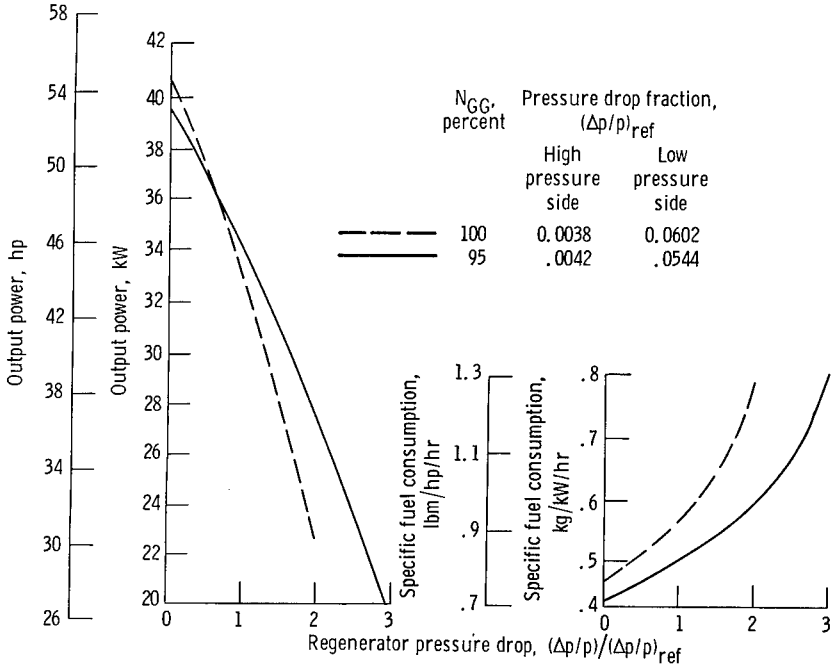

Figure 12. - Effect of regenerator pressure drop on power and specific fuel consumption. Gas generator speed, 46 800 rpm, 80 percent; power turbine speed, 30 030 rpm; power turbine discharge temperature, 1021 K (1837° R).

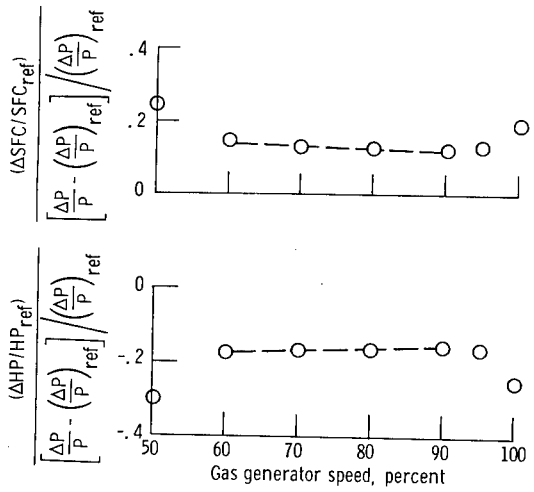

Figure 13. - Power and specific fuel consumption influence coefficients for reduced regenerator pressure drop.

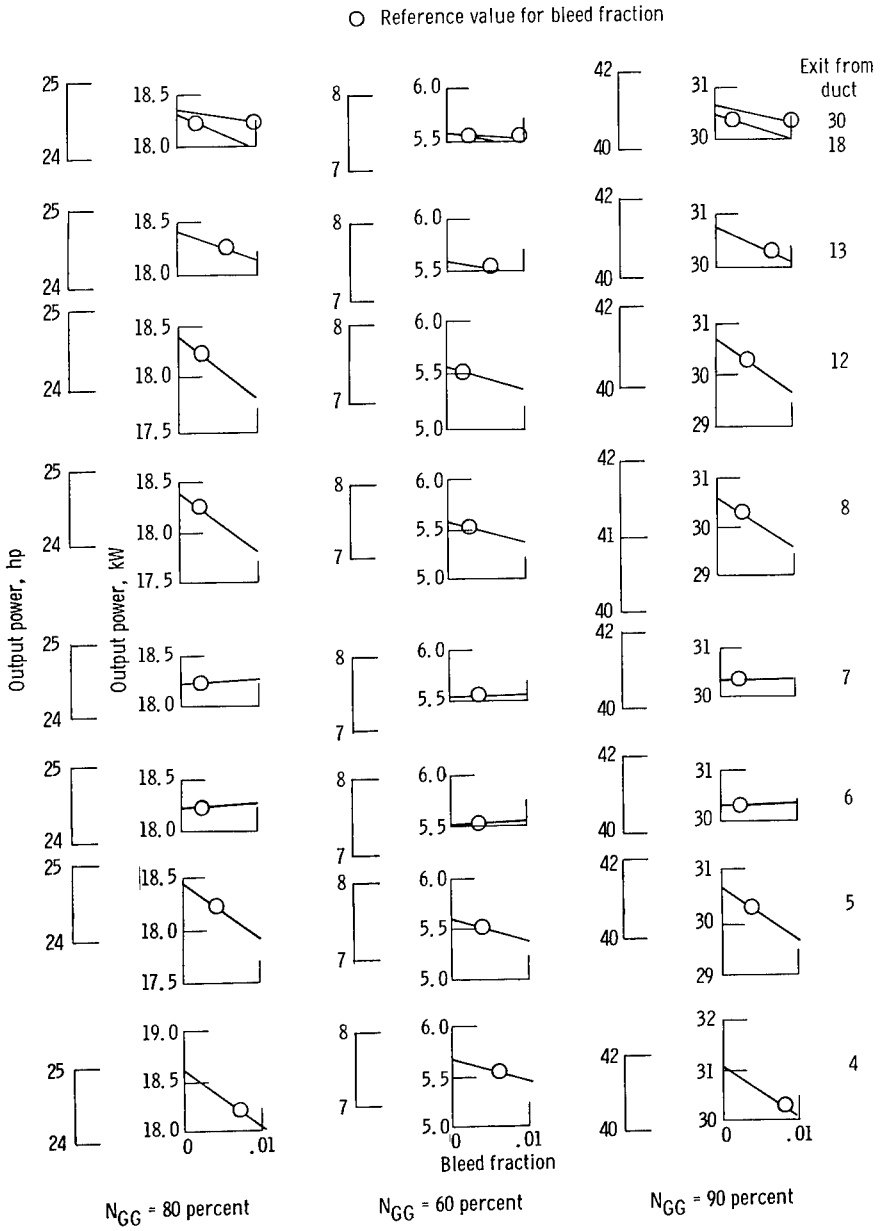

Figure 14. - Effect of various flow leaks on power.

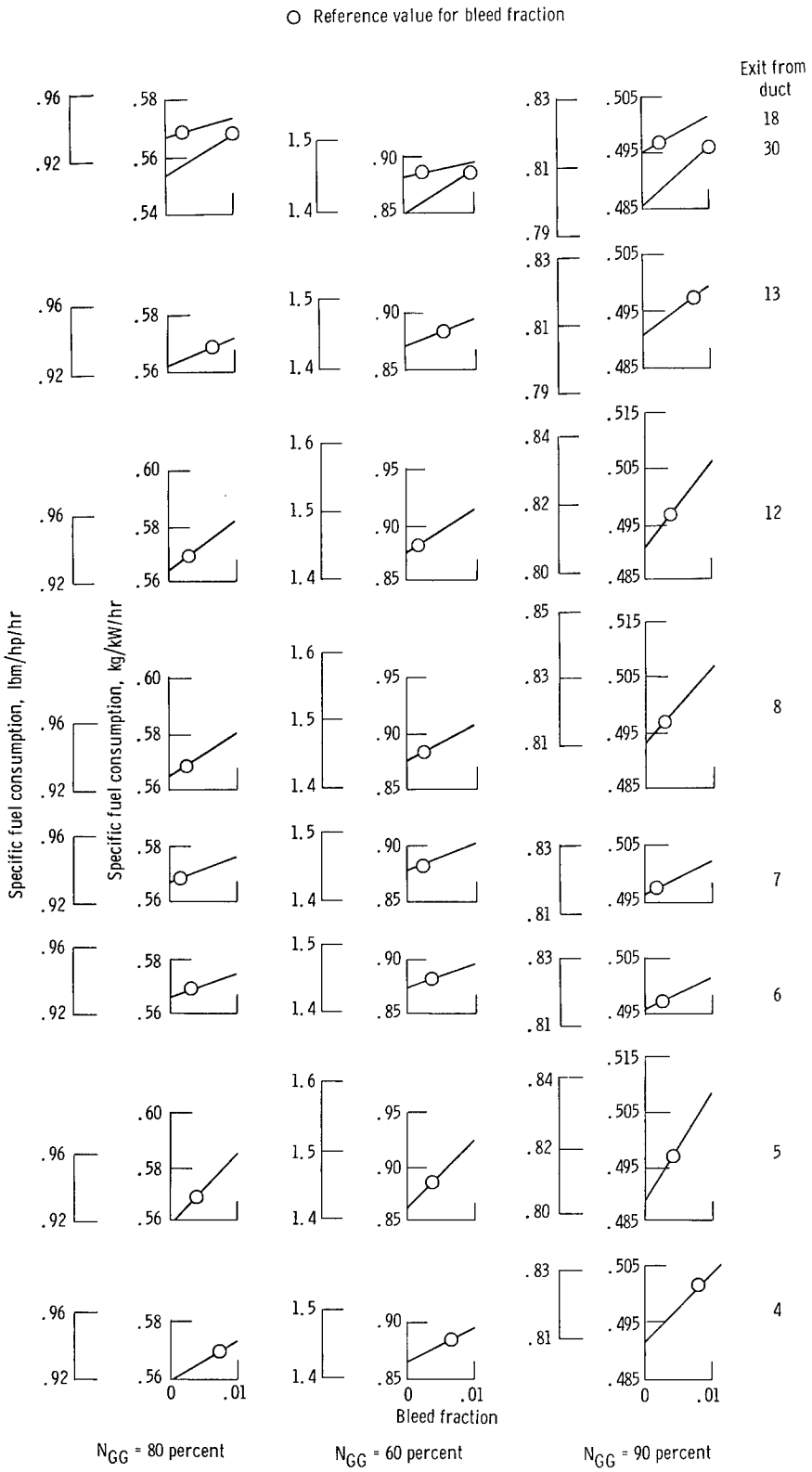

Figure 15. - Effects of various flow leaks on specific fuel consumption.

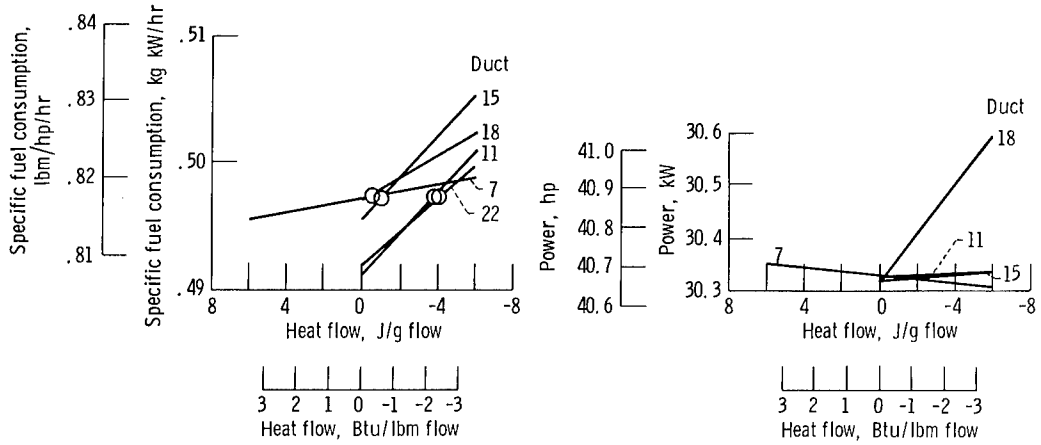

(a) Gas generator speed, 90 percent.

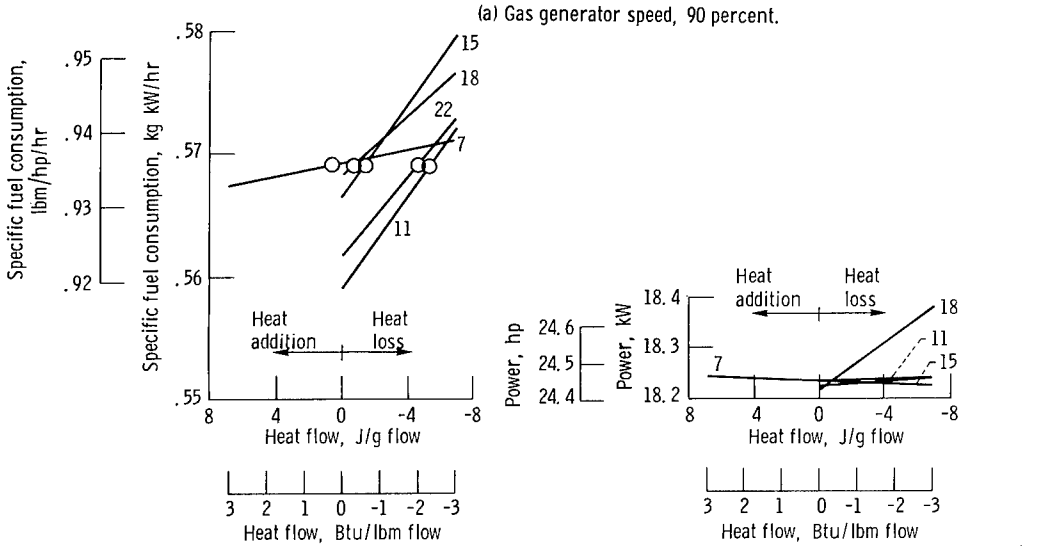

(b) Gas generator speed, 80 percent.

Figure 16. - Effect of various heat leaks on specific fuel consumption and engine power.

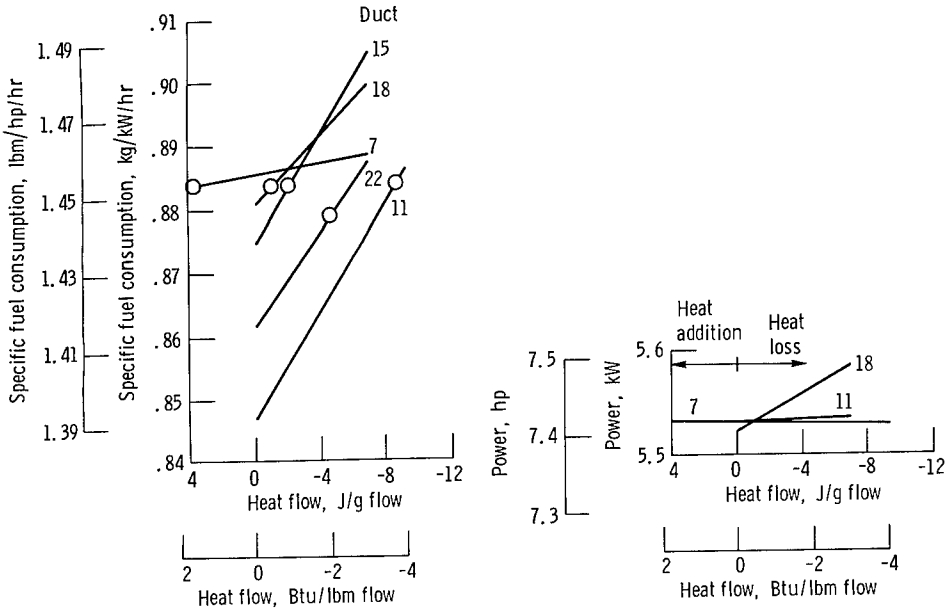

(c) Gas generator speed, 60 percent.

Figure 16. - Concluded.

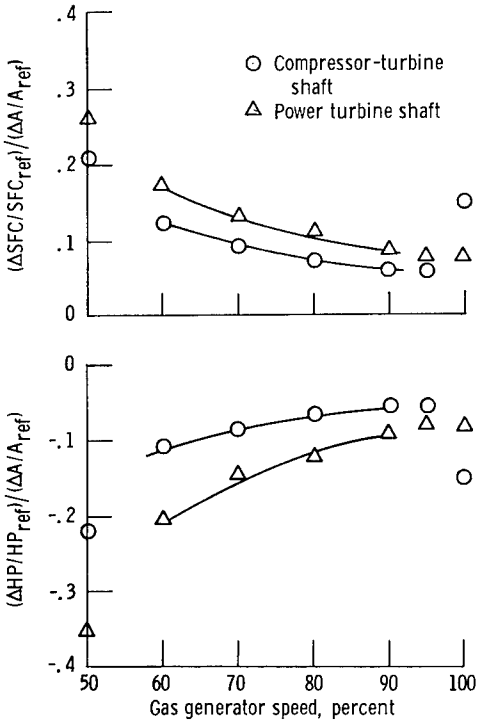

Figure 17. - Power and specific fuel consumption influence coefficients for reductions of gas generator and power turbine shaft parasitic power losses.

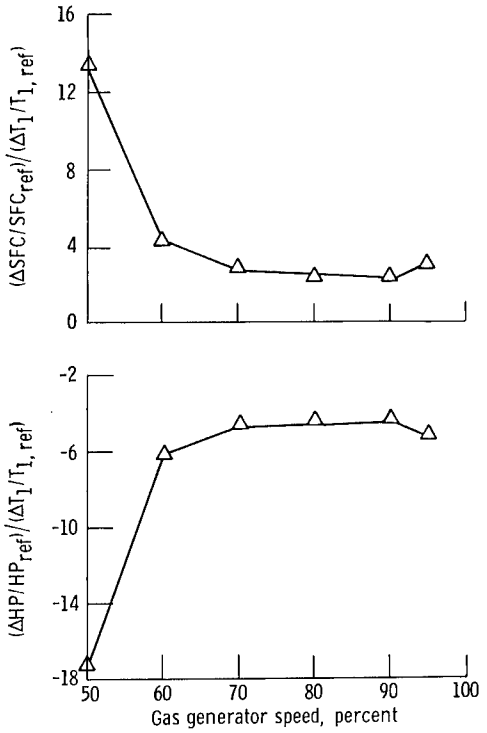

Figure 18. - Power and specific fuel consumption influence coefficients for changes of compressor inlet temperature. Constant power turbine discharge temperature, 1021 K (1837° R).

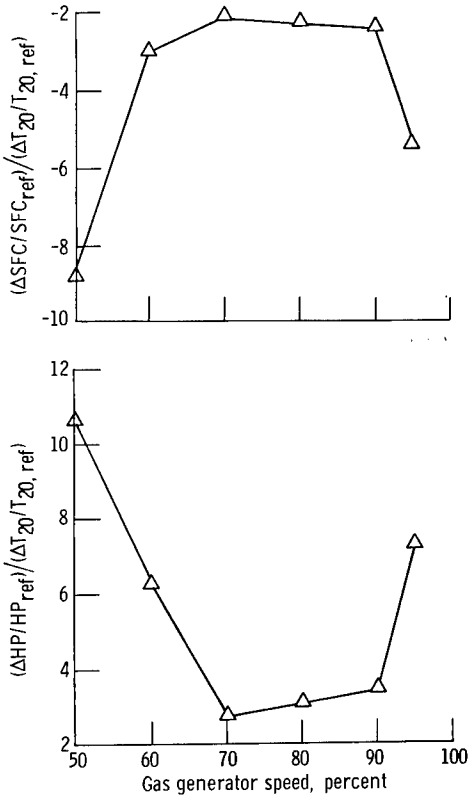

Figure 19. - Power and specific fuel consumption influence coefficients for increased power turbine discharge temperature. Constant compressor inlet temperature, 303 K (544.7° F).

1. Report No. NASA TM-79242	2. Government Accession No.	3. Recipient's Catalog No.
4. Title and Subtitle PERFORMANCE SENSITIVITY ANALYSIS OF DEPARTMENT OF ENERGY - CHRYSLER UPGRADED AUTOMOTIVE GAS TURBINE ENGINE (S/N 5-4)		5. Report Date December 1979 6. Performing Organization Code
7. Author(s) Roy L. Johnsen		8. Performing Organization Report No. E-147 10. Work Unit No.
9. Performing Organization Name and Address National Aeronautics and Space Administration Lewis Research Center Cleveland, Ohio 44135		11. Contract or Grant No.
12. Sponsoring Agency Name and Address U.S. Department of Energy Transportation Energy Conservation Division Washington, D.C. 20545		13. Type of Report and Period Covered Technical Memorandum 14. Sponsoring Agency ~~Code~~ Report No. DOE/NASA/1040-79/9

15. Supplementary Notes

Final report. Prepared under Interagency Agreement EC-77-A-31-1040.

16. Abstract

The performance sensitivity of a two-shaft automotive gas turbine engine to changes in component performance and changes to cycle operating parameters was examined. The engine tested was the Chrysler Upgraded engine developed under a U.S. Department of Energy contract. A test of one Upgraded engine at the NASA Lewis Research Center was one aspect of a corrective action program to remedy a power shortfall in the early development engines. To support that test, the engine was modeled for use with a computer performance prediction code. Performance sensitivity to turbomachinery efficiencies, regenerator effectiveness and pressure drop, parasitic losses, and flow and heat leaks was examined.

17. Key Words (Suggested by Author(s))	18. Distribution Statement
Automotive engines; Gas turbine engines; Influence coefficients; Sensitivity analysis	Unclassified - unlimited STAR Category 37 DOE Category UC-96

19. Security Classif. (of this report)	20. Security Classif. (of this page)	21. No. of Pages	22. Price*
Unclassified	Unclassified	34	$4.50

* For sale by the National Technical Information Service, Springfield, Virginia 22161

NASA-Langley, 1979

National Aeronautics and
Space Administration

Washington, D.C.
20546

Official Business
Penalty for Private Use, $300

THIRD-CLASS BULK RATE

Postage and Fees Paid
National Aeronautics and
Space Administration
NASA-451

12 1 1U,D, 020880 S00939DU
DEPT OF THE ARMY
ARMY TANK-AUTOMOTIVE COMMAND
RD&E DIRECTORATE
ATTN: TECHNICAL LIBRARY DRDTA-UL
WARREN MI 48090

NASA

POSTMASTER: If Undeliverable (Section 158 Postal Manual) Do Not Return